Investigation and Performance Enhancement of the Empirical Mode Decomposition Method Based on a Heuristic Search Optimization Approach

Yannis Kopsinis, *Member IEEE,* and Steve McLaughlin, *Senior Member IEEE,*

Abstract

Empirical mode decomposition (EMD) is a relatively new, data-driven adaptive technique for analyzing multicomponent signals. Although it has many interesting features and often exhibits an ability to decompose nonlinear and non-stationary signals, it lacks a strong theoretical basis which would allow a performance analysis and hence the enhancement and optimization of the method in a systematic way. In this paper, the optimization of EMD is attempted in an alternative manner. Using specially defined multicomponent signals, the optimum outputs can be known in advance and used in the optimization of the EMD free parameters within a genetic algorithm framework. The contributions of this paper are twofold. Firstly, the optimization of both the interpolation points and the piecewise interpolating polynomials for the formation of the upper and lower envelopes of the signal reveal important characteristics of the method which where previously hidden. Secondly, basic directions for the estimates of the optimized parameters are developed, leading to significant performance improvements.

I. INTRODUCTION

The method of Empirical mode decomposition (EMD), introduced by Huang et. al. [1], aims to analyze multicomponent signals [2] by breaking them down into a number of elementary amplitude and frequency

modulated (AM/FM) zero mean signals termed intrinsic mode functions (IMFs). Recently EMD has received much attention due to its interesting features. Among others, the most significant of them are:

- It can be applied and provide useful and reliable results regardless of the non-stationary and/or nonlinear characteristics of the signal under consideration.

- The elementary signals are virtually monocomponent (narrowband) leading to meaningful instantaneous frequency estimates via the Hilbert transform or other alternative techniques [3].

- EMD results in an adaptive signal-dependent time-variant filtering procedure able to directly extract signal components which significantly overlap in time and frequency [4].

- The physical meaning of the intrinsic processes underlying the complex signal is often preserved in the decomposed signals. This is mainly due to the fact that the results are not prejudiced by pre-determined basis and/or subband filtering processes.

As was pointed out in [5] EMD considers signals as "fast oscillations superimposed on slow oscillations". The task of EMD is to iteratively reveal locally the slow oscillating part of the signal according to a procedure called sifting which involves the computation of the upper and lower envelopes which *enfold* the fast oscillating signal. The envelopes are usually spline functions which interpolate some predefined points of the fast oscillating signal called interpolation points. The IMFs result from the successive subtraction of the estimated slow oscillating signals from the multicomponent signal. After the extraction of an IMF, the same procedure is repeated with the residual. Although the validity and the robustness of EMD have been shown in a number of applications [6], [7], [8], the EMD technique lacks a well established theoretical analysis which would permit a convergence proof and a direct, systematic optimization of the method. Due to the nature of EMD and the obscure way it operates, the so far published modifications of the initially proposed algorithm leading to performance improvement are limited [4], [9].

The best spline implementation is one of the most important open problems related to the EMD method [10]. Moreover, another crucial issue which is related not only to the EMD performance enhancement but also to the better understanding of the way the decomposition is realized, is the detection of the optimum positions of the interpolation points. So far, the investigation of EMD has been realized in two different ways. Either empirically, based on simulation examples and specific-heuristically defined configurations of the EMD; or by drastically modifying the sifting procedure [11] of the method, [12] in order for the EMD to be more easily approached analytically but, usually by compromising the performance. Moreover, the EMD behaviour when analyzing stochastic noise-like signals has also been examined allowing important conclusions to be drawn about the filtering characteristics of the algorithm [13].

In this paper an alternative procedure is followed. EMD is examined by using appropriately designed multicomponent signals which allow as to know explicitly the optimum outputs that the EMD should "ideally" provide. The knowledge of the desired EMD outputs, is pivotal in allowing the use of advanced techniques for the optimization of the parameters of the method which determines its behaviour. The contribution of the paper is twofold. Primarily, to facilitate our understanding of the inherent way that EMD succeeds in decomposing signals. Secondly, to propose new methods for both interpolation points estimation and envelope formulation that exploit the new findings and could serve as a starting point for novel, efficient EMD variants. More specifically, the optimization procedure shows that there are specific extrema, which are related to the signal that is to be extracted, and are able to lead to much improved decomposition performance if the extrema of EMD are set to them. As a result, EMD can be understood as a procedure that attempts to iteratively converge to those optimized extrema. Furthermore, by adopting the optimized extrema, the EMD envelopes tend to be tangential to the processed signal. Based on the observations above, signal preprocessing methods leading to interpolation points estimates closer to optimized ones are proposed. Finally, a type of Hermitian interpolation is also proposed which succeeds in preserving the characteristics of the optimized envelopes.

The remainder of the paper is organized as follows. In section II the basics of EMD together with the modifications and formulations which allow the utilization of optimization techniques are presented. Section III describes the use of a GA for the optimization of the interpolation points and the way that the corresponding results can be exploited for the development of enhanced interpolation points estimators. In a similar manner, the optimized interpolant is estimated and a new interpolation method is proposed in section IV. Section V deals with the application of EMD configured with the standard and the proposed ways to a number of simulation examples. Conclusions are then drawn in section VI.

II. EMD ALGORITHM

EMD aims to decompose a multicomponent signal $x(t)$ into a number of virtually monocomponent IMFs $h(t)$, plus a non zero-mean low order polynomial remainder $r(t)$:

$$x(t) = \sum_{i=1}^{N} h^{(i)}(t) + r(t). \tag{1}$$

Each one of the IMFs, e.g. $h^{(k+1)}$, is obtained by applying a process called sifting to the residual multicomponent signal as in the equation below

$$x^{(k)}(t) = x(t) - \sum_{i=1}^{k} h^{(i)}(t). \tag{2}$$

The sifting process is an iterative procedure which aims to achieve improved estimates of $h^{(k)}(t)$ in each iteration. More specifically, during the $(n+1)$th sifting iteration, the temporal estimate of the IMF, $\hat{h}_n^{(k)}(t)$, obtained in the previous sifting iteration, is processed according to the following steps (some of the quantities derived are shown in Fig. 1):

1) Specify some time instances $\boldsymbol{\tau_u} = [\tau_{u,1}, \ldots, \tau_{u,M}]$, $\boldsymbol{\tau_l} = [\tau_{l,1}, \ldots, \tau_{l,L}]$ called nodes and the corresponding IMF values $\hat{\mathbf{h}}_{u_n}^{(k)} = [\hat{h}_n^{(k)}(\tau_{u,1}), \ldots, \hat{h}_n^{(k)}(\tau_{u,M})]$, $\hat{\mathbf{h}}_{l_n}^{(k)} = [\hat{h}_n^{(k)}(\tau_{l,1}), \ldots, \hat{h}_n^{(k)}(\tau_{l,L})]$ called interpolation points. These points are utilized in the formation of two envelopes, an upper and a lower one, which enfold the temporal estimate $\hat{h}_n^{(k)}$. The interpolation points are determined according to some criteria, e.g. to be the maximum extrema of $\hat{h}_n^{(k)}(t)$ for the upper envelope case ($\boldsymbol{\tau_u} = \{t: \dfrac{d\hat{h}_n^{(k)}(t)}{dt} = 0, \dfrac{d^2\hat{h}_n^{(k)}(t)}{dt^2} < 0\}$) and the minimum extrema for the lower case ($\boldsymbol{\tau_l} = \{t: \dfrac{d\hat{h}_n^{(k)}(t)}{dt} = 0, \dfrac{d^2\hat{h}_n^{(k)}(t)}{dt^2} > 0\}$).

2) Interpolate, according to a predetermined scheme, (e.g. natural cubic spline interpolation), between the points defined in the first step discussed above in order to form the upper $I_{\tau_u}(t)$ and the lower envelopes $I_{\tau_l}(t)$.

3) Compute the *mean envelope* $m_{n+1}^{(k)}(t) = (I_{\tau_u}(t) + I_{\tau_l}(t))/2$.

4) Obtain the refined estimate of the IMF as $\hat{h}_{n+1}^{(k)}(t) = \hat{h}_n^{(k)}(t) - m_{n+1}^{(k)}(t)$ and proceed from step 1 again for the next iteration unless a stopping criterion has been fulfilled. If the stopping criterion is fulfilled, then set $h^{(k)}(t) = \hat{h}_{n+1}^{(k)}(t)$ and proceed to the next IMF.

For the first iteration, the residual signal $x^{(k-1)}(t)$ is used as initial IMF estimate $\hat{h}_1^{(k)}(t)$ and $x^{(0)}(t) = x(t)$. Alternatively, instead of computing an upper and a lower envelope, the direct estimation of the mean envelope can be realized by interpolating the successive inflection points of $\hat{h}_n^{(k)}(t)$, i.e., $\{t: \dfrac{d^2\hat{h}_n^{(k)}(t)}{dt^2} = 0\}$ or, in the first iteration, of the residual signal $x^{(k-1)}(t)$). Hereafter, the latter EMD variant will be called direct mean EMD (DMEMD) in order to differentiate it from the standard algorithm for EMD [1]. Ideally, the final result of each sifting process is the extraction of the faster oscillations preserving at the same time their amplitude. For example, consider the case where the complex signal consists of N AM-FM modulated monocomponent signals

$$x(t) = \sum_{i=1}^{N} s_i(t) = \sum_{i=1}^{N} \alpha_i(t)\cos(\phi_i(t)), \tag{3}$$

with instantaneous frequencies (IF) $f_i(t) = \frac{1}{2\pi}\frac{d\phi_{a,i}(t)}{dt}$, where $\phi_{a,i}(t)$ denotes the phase of the ith corresponding analytic signal written in complex polar coordinates. In this scenario, EMD should be able to extract, at any time instant, this signal out of N that locally has a highest IF. Under the assumption
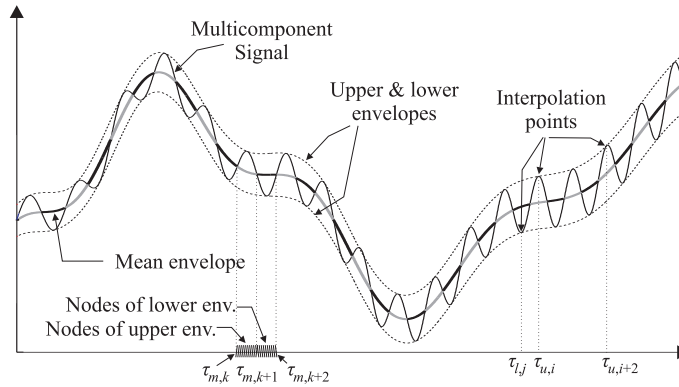
Fig. 1. A multicomponent signal together with several quantities related to the EMD method.

of $f_i(t) > f_j(t)$ for any $i < j$ and for all time instances t, the ith desired estimated IMF, $h^{(i)}(t)$, has to be equal to $s_i(t)$. The above assumption will now be adopted since it does not affect the analysis or the findings of this work which are still valid in the case of frequency-overlapped signal components. Moreover, the knowledge of the desired EMD outputs, i.e. the monocomponent signals $s_i(t)$, allows for the adaptive optimization of EMD, and important conclusions to be drawn.

The estimate of $h^{(k)}(t)$ after n sifting iterations can be described mathematically as follows

$$
\begin{aligned}
\hat{h}_1^{(k)}(t) &= x^{(k-1)}(t) - m_1^{(k)}(t) \\
\hat{h}_2^{(k)}(t) &= \hat{h}_1^{(k)}(t) - m_2^{(k)}(t) \\
&\vdots \\
\hat{h}_n^{(k)}(t) &= \hat{h}_{n-1}^{(k)}(t) - m_n^{(k)}(t)
\end{aligned}
\tag{4}
$$

which can be written as

$$
\begin{aligned}
\hat{h}_n^{(k)}(t) &= x^{(k-1)}(t) - (m_1^{(k)}(t) + m_2^{(k)}(t) + \ldots + m_n^{(k)}(t)) \\
&= x^{(k-1)}(t) - M_n^{(k)}(t),
\end{aligned}
\tag{5}
$$

with $M_n^{(k)}(t)$ defined here as the *total mean envelope*. Equation (5) reformulates the sifting process as an iterative procedure for the estimation of the slow oscillating *local mean* of the multicomponent signal which is a perspective that offers certain advantages as will become clear in the sequel. Assuming that the decomposition is accurate up to the $(k-1)$ th signal, i.e., $h^{(i)}(t) = s_i(t)$, $i = 1, \ldots, k - 1$ then

from (2),(3), the residual signal is known in advance and is equal to

$$x^{(k-1)}(t) = \sum_{i=k}^{N} s_i(t). \tag{6}$$

So, the optimum total mean envelope which leads to the accurate decomposition of the kth signal, i.e., $h^{(k)}(t) = x^{(k-1)}(t) - M_{opt}^{(k)}(t) = s_k(t)$, is given by the sum of the signals with the lower IFs up to the signal to be extracted:

$$M_{opt}^{(k)}(t) = \sum_{i=k+1}^{N} s_i(t). \tag{7}$$

The intersection points between the optimum mean envelope and the residual signal provide useful information with respect to the optimization of the method:

$$\begin{aligned} \boldsymbol{\tau_m} &= [\tau_{m,1}, \ldots, \tau_{m,Q}] \\ &= \{t: \ M_{opt}^{(k)}(t) = x^{(k-1)}(t)\}, \end{aligned} \tag{8}$$

which consequently can be rewritten as

$$\boldsymbol{\tau_m} = \{t: \ s_k(t) = 0\}. \tag{9}$$

In the case of DMEMD these interpolation points of the mean envelope would be the optimum ones. In other words, the optimum interpolation points $\boldsymbol{\tau_m}$ depend on the signal, $s_k(t)$, that we are trying to extract. This observation can explain the difficulties and inaccuracies which arise in the case of DMEMD when the mean envelope is estimated directly through the inflection points and at the same time the sifting process is replaced by a partial differential equation-based formulation [11]. The latter method, forces a piecewise cubic polynomial curve to interpolate the inflection points of the residual signal $x^{(k-1)}$. Unfortunately, the inflection points can deviate considerably from the optimum interpolation points which, as noted before, are exclusively determined by the zero-crossing points of the signal that is to be extracted.

In this paper the focus is on standard algorithm for EMD [1], and a question that arises is:

Are there optimum interpolation points having specific properties in the standard EMD case? If yes, how well are they approximated by the *local extrema*, i.e. the maximum and minimum extrema which are usually adopted in practice? The answer to these questions is not as straightforward as in the DMEMD case. However, $\boldsymbol{\tau_m}$ can reveal the possible positions of the optimum interpolation points.

The interpolation points of the upper and the lower envelope, should be selected in a way capable of leading to estimated mean envelope equal to $M_{opt}^{(k)}(t)$. At the same time, the upper and the lower envelope should be over and under the mean envelope respectively. Investigating Fig. 1, it can be argued that, each one of the intervals $(\tau_{m,i}, \tau_{m,i+1})$ can only contain interpolation points which belong exclusively to either

the upper or the lower envelope depending on whether the residual signal is "over" or "under" $M_{opt}^{(k)}(t)$. In Fig. 1, the intervals that correspond to upper or lower envelopes are shown with light or dark colored mean envelope respectively. In the next section, the optimum interpolation points will be detected by means of a genetic algorithm (GA) heuristic search procedure [14].

III. DETECTION OF THE BEST INTERPOLATION POINTS

A. Genetic Algorithms

The GA is a searching process based on the laws of natural selection and genetics [15]. The basic elements of a GA are the chromosomes $\chi_i = [g_{i,1}, \ldots, g_{i,n}]$, $i = 1 \ldots N$, with each one of them containing n genes where n is the number of the unknown parameters with respect to which the optimization will occur. The set of N chromosomes constitutes a generation and each chromosome represents a possible solution to the problem. The GA is iteratively searching for the best or "fitter" chromosome, i.e. for the best parameter set, through a number of successive generations which are created based on evolutionary strategies which guarantee that the fitter chromosomes have greater chances to survive.

From an initial, randomly generated, population of chromosomes, a group of them is dedicated to be the parents of the next generation according to a selection strategy which evaluates the fitness of each chromosome. The fitness is computed via an error function which is problem specific. The offspring, is generated through the crossover and mutation operations and the fittest of them replaces some of the chromosomes in the current population leaving the size of the population constant during the procedure. The GA cycle is repeated until the fittest chromosome remain constant for a specific number of successive generations. In the applications of the GA which will follow, *tournament selection* and *multipoint crossover* have been adopted.

B. EMD optimization: Best interpolation points detection

In section II it was seen that the use of appropriately designed multicomponent signals allow us to know in advance the optimum outputs of the EMD method and consequently the intervals along the time axes with nodes which explicitly correspond to either the upper or the lower envelope. This fact will be exploited in order to efficiently select the best ones among all the possible interpolation points by means of a GA-based search procedure. It must be emphasised, that a modified EMD with the GA embedded in it is **not** being proposed here. *The GA is simply a means to investigate the way that EMD processes the signals in order to reveal directions leading to both performance enhancement and insight that would*

aid theoretical analysis of the method. Hereafter, with respect to the GA-based examination of EMD, the focus will be only on the extraction of the first IMF since the procedure is valid for all others.

Consider that there are M intervals that are able to contain upper envelope nodes $T_{u,k} = \{(\tau_{m,i}, \tau_{m,i+1}), i : M_{opt}^{(1)}(t) < x(t)$ for $t \in (\tau_{m,i}, \tau_{m,i+1})\}$, $1 \leq k \leq M$ and L intervals that are able to contain lower envelope nodes $T_{l,n} = \{(\tau_{m,i}, \tau_{m,i+1}), i : M_{opt}^{(1)}(t) > x(t)$ for $t \in (\tau_{m,i}, \tau_{m,i+1})\}$, $1 \leq n \leq L$. Also assume that in each interval there is explicitly one node[1]. It is easy to realize that this assumption in general results in a number of nodes similar or somewhat larger than that which results from the standard local extrema case. The optimization which is accomplished with the aid of the GA is as follows: Minimize the relative error between the actual mean envelope $M_{opt}^{(1)}(t)$ and the estimated total mean envelope $M_n^{(k)}(t)$ after a preset number of n sifting iterations with respect to the adopted upper and lower envelope node vectors $\boldsymbol{\tau_u}$ and $\boldsymbol{\tau_l}$ respectively.

The ith chromosome in the adopted GA has the form $\chi_i = [\tilde{\tau}_{u,1}, \tilde{\tau}_{u,2}, \ldots, \tilde{\tau}_{u,M}, \tilde{\tau}_{l,1}, \tilde{\tau}_{l,2}, \ldots, \tilde{\tau}_{l,L}]$, where $\tilde{\tau}_{\cdot,k}$ denotes a random value in the interval $T_{\cdot,k}$. The fitness function comprises a number of steps:

- Split the chromosome in the upper and lower envelope node vectors $\boldsymbol{\tau_u}$ and $\boldsymbol{\tau_l}$ and compute the corresponding interpolation points.

- Perform n times the sifting iteration steps 2 and 3 (see section II) using in each iteration the same nodes as were defined by the chromosome under consideration in order to estimate the total mean envelope $M_n^{(1)}(t)$ from (5).

- Compute the chromosome fitness with the following error function[2]:

$$
\begin{aligned}
F \;=\; & \int |M_{opt}^{(1)}(t) - M_n^{(1)}(t)|dt + \\
& \int_{t:I_{\tau_u}(t) < h_{n-1}^{(1)}(t)} |h_{n-1}^{(1)}(t) - I_{\tau_u}(t)|dt + \\
& \int_{t:I_{\tau_l}(t) > h_{n-1}^{(1)}(t)} |h_{n-1}^{(1)}(t) - I_{\tau_l}(t)|dt
\end{aligned}
\tag{10}
$$

The first term deals with the main objective of the optimization procedure, i.e. to provide accurate mean envelope estimates, while the second and the third terms prevent the GA from converging to trivial solutions, e.g., both envelopes to coincide close to the optimum mean envelope. In fact

---

[1]The procedure explained here has also been realized for multiple nodes per interval leading to roughly the same conclusions as in the single node case.

[2]Here the general expression dealing with analog signals is given. However, in practice a sampled version of the signals examined is used so the integrals are substituted with the corresponding summations.

these last two terms guarantee that the interpolation functions will be envelopes which will *"tightly include"* the processed signal.

C. GA application to EMD

The time-frequency representation of the multicomponent signal adopted here is shown in Fig. 2 together with the three monocomponent signals which it comprises. Moreover, the multicomponent signal together with the optimum mean envelope are shown in Fig. 3a in the time domain. In this first example,
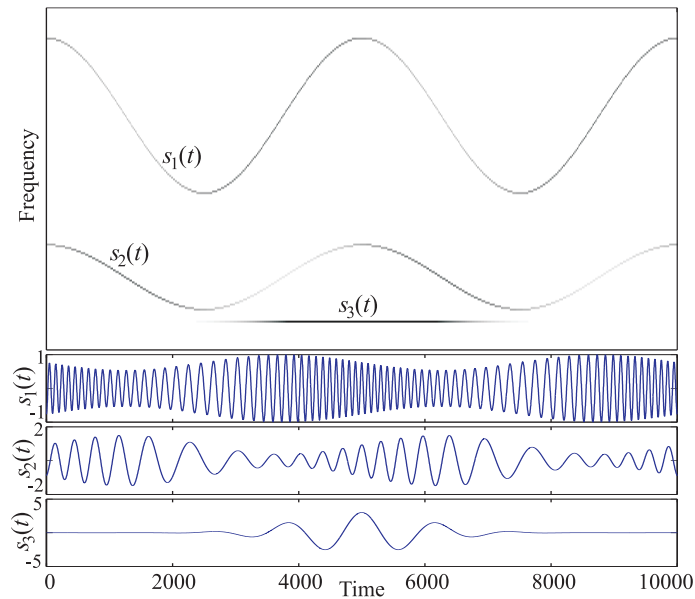

Fig. 2.   Complex signal comprising three amplitude and frequency modulated signals.

the higher frequency monocomponent signal has been intentionally chosen to be well separated from the rest of the signals. The GA is used in order to detect the upper and lower envelope nodes that optimize the extraction of the first monocomponent signal after a predetermined number of n sifting iterations. The GA-based optimization of the interpolation points was realized based on cubic splines and $n = 5$ sifting iterations. Fig. 3(b-c) shows the error along the time axis between the optimum and the estimated mean envelope of the signal when the latter has been obtained after one sifting iteration applied to the signal depicted in Fig. 3a. The dark blue and the dark red areas correspond to low and high error respectively as can be seen from the corresponding color-error map (Fig. 3d), which relates to all similar figures in the paper. The error-bars correspond to 3rd and 5th order spline interpolation and differently obtained local extrema, namely, GA-optimized (error-bars b1 and c1), extrema of the highest
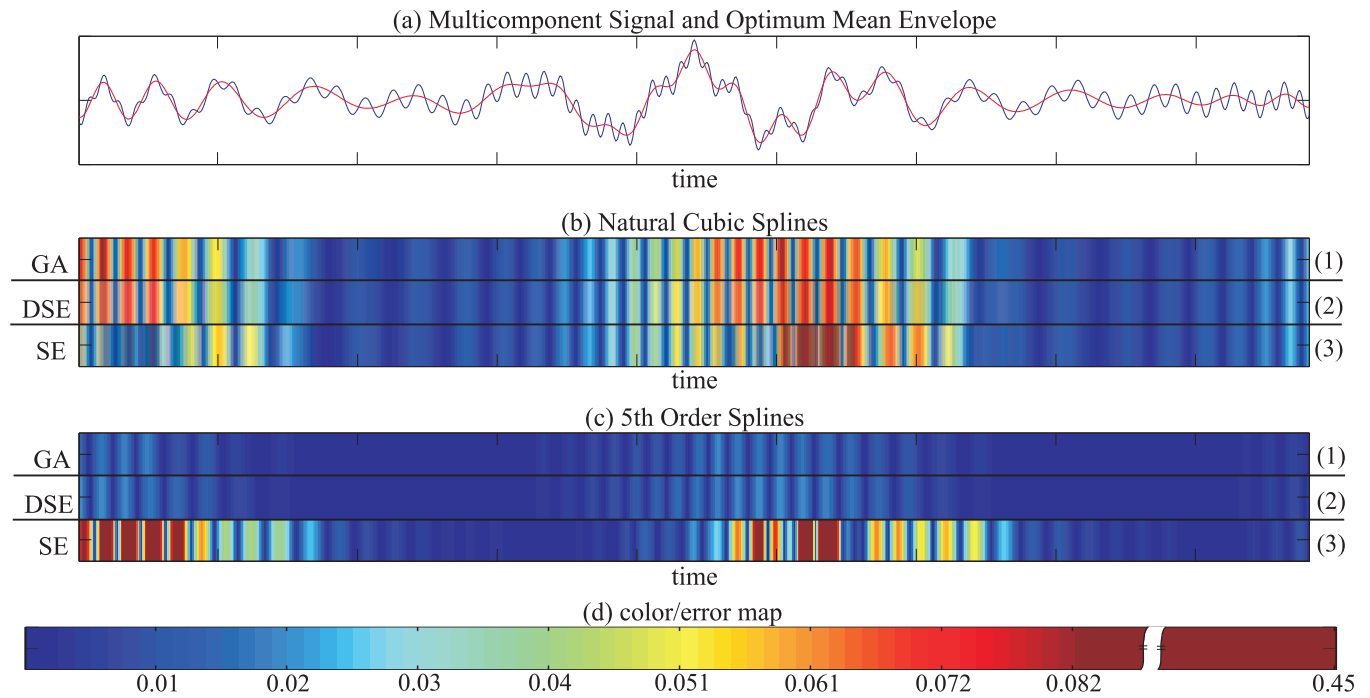
Fig. 3. Relative error between the estimated, after 1 sifting iteration, and the actual mean envelope (red curve in (a)) during the first IMF extraction from the signal shown with blue curve in (a). The error bars correspond to different spline orders and interpolation points obtained from genetic algorithm optimization (GA), extrema of the desired high frequency signal (DSE) and local extrema of the multicomponent signal (SE).

instantaneous frequency monocomponent signal which is the one that optimally should be extracted (b2 and c2) and local extrema (b3 and c3) which have been used in EMD to date. It can be easily observed that the optimized interpolation points estimated by the GA virtually coincide with the extrema of the signal which is about to get extracted, i.e., the multicomponent signal of the highest frequency. Hereafter, we will refer to the extrema, nodes and interpolation points of the desired signal to be extracted as *desired* and to the extrema, nodes and interpolation points estimated by a GA procedure as *optimized*.

Fig. 4(b-d) shows the improvement achieved with five sifting iterations for the three interpolation points selection methods, compared to the one-sifting iteration and desired interpolation points case shown in Fig. 4a. In the case of Fig. 4d which corresponds to the standard EMD method, the local extrema of the multicomponent signal are recomputed in each sifting iteration, while in the cases of the optimized (Fig. 4c) and desired extrema (Fig. 4b), the same interpolation points are used in every iteration. This illustrates the power of EMD, which although adopting interpolation points far from the desired ones, it iteratively succeeds in gradually improving estimates while approaching to the desired interpolation points. When
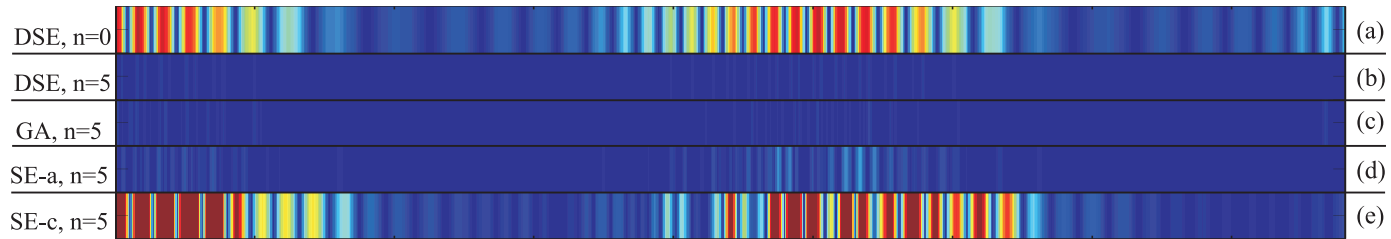
Fig. 4. Relative error between the estimated and the actual mean envelope during the first IMF extraction. The first two error bars correspond to interpolation points obtained from the local extrema of the desired high frequency signal and one or five sifting iterations respectively, the third error bar corresponds to GA optimized points and 5 iterations and the last two error bars correspond to local extrema reobtained in each iteration or just estimated before the first sifting respectively. The error map of Fig. 3 applies here as well.

the extrema obtained from the multicomponent signal at the first sifting serve as interpolation points throughout the rest of the sifting iterations, the results are disappointing (see Fig. 4(e)).

The findings of this subsection are not totally unexpected. The essence of EMD is to identify the oscillatory mode that corresponds to the high frequency signal by its characteristic time scales in the residual signal [16]. The time scales of a signal are determined by the distance between its characteristic points such as zero crossing points or extremes. It is not surprising, that the EMD method performs better when it is directly supplied with the characteristic points of the fast oscillating signal.

In practice, neither the extrema of the desired signals are known, nor can they be estimated with the aid of a GA. The maxima and minima of the multicomponent signal serve as estimates to the desired interpolation points and it should be expected that the closer the estimated extrema are to the desired ones the better the decomposition performance is. The challenge is to find ways of estimating the desired interpolation points from the multicomponent signal more accurately than the standard extrema method does. The development of optimized methods for the interpolation points is beyond the scope of this paper. However, a discussion on the possible directions that could be followed and the likely difficulties which may arise is attempted in the next subsection.

D. New interpolation points estimation techniques

In many cases the extrema of the multicomponent signal fail to approach the extrema of the desired highest instantaneous frequency signal and, to make matters worse, there are circumstances where extrema can be missed, i.e transformed to smooth riding waves [1]. The appropriate preprocessing of the multicomponent signal in order to enhance its high frequency component leads to local extrema which

are closer to the desired interpolation points. Here, two such preprocessing methods are briefly examined. The differentiation and the high pass filtering method.

The fast oscillating signal enhancement goal can be realized with differentiation. For example, the second derivative of the multicomponent signal is able to track the changes of the faster oscillating signal better because the latter is characterized from faster *acceleration*. Moreover, the local extrema of even order derivatives of the multicomponent signal are more likely to be closer to the desired extrema than the extrema of the multicomponent signal itself. A sketch proof is outlined in appendix I for the case of signals comprising both constant amplitude and frequency monocomponent signals. The potential of using the local extrema of higher order derivatives of the multicomponent signal has already been reported [17]. However, the authors' starting point was quite different, namely the form of the curvature of the signal which is given as a function of the first and the second derivative:

$$c(t) = \frac{d^2 x(t)/dt^2}{(1 + (dx/dt)^2)^{3/2}} \qquad (11)$$

Apparently, the relation between the curvature extrema and the differentiation method as means for estimating IPs closer to the desired ones provides a new viewpoint to the inherent function of the curvature extrema method.

There are a number of problems related to the application of higher-order derivatives in EMD. First, in the case of closely sampled signals, the machine precision can easily be overcome due to the subtractions involved in the numerically computed derivatives, leading to noise-like effects and "false" additional extrema. Interpolation of the signal samples before the differentiation can eliminate this problem. Second, it is well known that differentiation can result in noise amplification. Thus, differentiation has to be accompanied with some form of appropriate filtering, with Savitzky-Golay smoothing filter [18] and specialized wavelet techniques [19] being possible candidates. Additionally, the adoption of adaptive - smoothing splines [20] can be an extension of EMD in the presence of noise. Third, the use of derivatives can alter the meaning of certain signals such as intrawave frequency modulated signals [17]. Fourth, the existence of discontinuities and/or abrupt changes in slowly oscillating nonlinear signals can result in extrema that do not belong to the desired monocomponent signal. For all the cases above, it is an open issue to develop techniques that fit to and exploit the special characteristics of EMD. Fig. 5(b-e) shows the error (absolute time difference) between the desired nodes which correspond to the extrema of signal $s_1(t)$ of Fig. 5(a) and the nodes that correspond to the local extrema (b), the curvature extrema (c) the local extrema of the second derivative of the multicomponent signal (d) and the local extrema of the fourth derivative of the multicomponent signal (e). The filled circles in (b) denote missed extrema. For
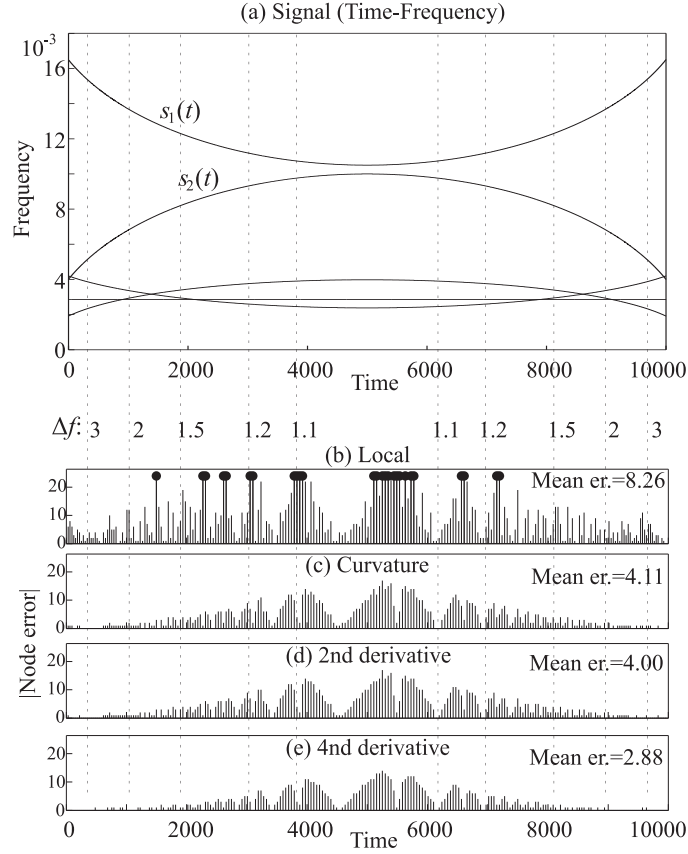
Fig. 5. Error in time instances between the optimum and the estimated nodes for several derivation-based nodes estimation schemes. Δf indicates the ratio of the frequency of signal $s_1(t)$ over the frequency of $s_2(t)$ along the time axis.

the numerical computation of the derivatives the central formula of order four:

$$f'(x) \approx \frac{-f(x + 2d) + 8f(x + d) - 8f(x - d) + f(x - 2d)}{12d}, \qquad (12)$$

was used with d being the sampling period which was chosen low enough in order to prevent the production of round-off errors during the differentiation. Observe that the differentiation leads in general to more accurate estimates with the second derivative and the curvature method exhibiting similar performance.

Apart from the high frequency enhancement methods based on differentiation, it is possible to resort to high pass filtering methods. The extrema of the filtered multicomponent signal are expected to lie closer to the desired ones due to the fact that the energy of the lower frequency signals which are responsible for the shifting or even the hiding of the observed extrema will be decremented. Still this proposed direction for interpolation points estimation is accompanied by a number of difficulties and is open to research

issues. First of all, the group delay that the filter introduces to the processed data must be known since it will result in a further shifting of the observed extrema. Linear phase finite impulse response (FIR) filters lead to constant and easy to compute group delay. However, the long delay which they usually entail, may be a disadvantage for some applications. Second, it remains an open question as to how the filter cutoff frequency should be selected. To make things more complicated, the cutoff frequency may need to be adaptive and in a sense to "track" the frequency changes of the fast oscillating signal.
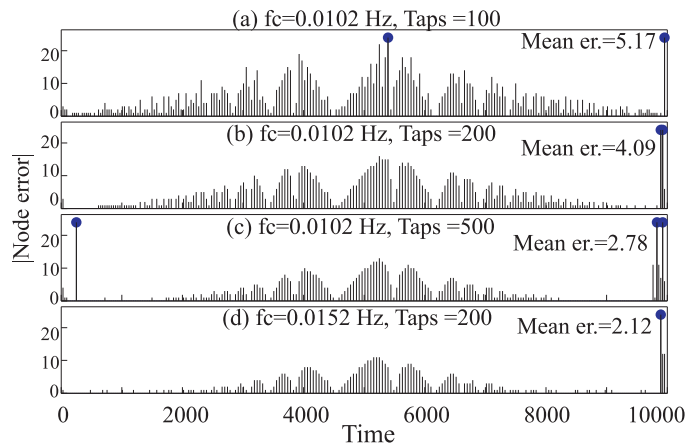

Fig. 6. Error in time instances between the optimum and the estimated nodes for several FIR filtering-based nodes estimation schemes.

Fig. 6 shows the estimation error for different configurations of an FIR filter applied to the signal of Fig. 5a. In the cases shown in Fig. 6(a)-(c), the cutoff frequency was set equal to the mid frequency point between signals $s_1(t)$ and $s_2(t)$ and the length of FIR filters was chosen to be 100, 200 and 500 taps respectively. Observe that the optimum extrema detection performance is in general improved with the increment of the filter lengths. However, the longer the filter length, the longer the group delay and the less the signal length which is effectively processed correctly. This is apparent from the errors which appear at the rightmost hand side of Fig. 6.

When it comes to the selection of the filter cutoff frequency the rules seem to be quite different from other filtering cases. The multicomponent signal is filtered not in order to isolate the high frequency signal but in order to "decontaminate" it from the low frequency ones. From this perspective, it may even be acceptable, if not required, to filter out large amounts of energy of the high frequency signal if this serves the extrema estimation. For example, in Fig. 6(d) where with only 200 taps, better performance than in the case of a 500 taps long filter is achieved by increasing the cutoff frequency by almost 50%, i.e. $D_f = 0.015$Hz.

IV. IMPROVED PIECEWISE INTERPOLATION METHODS

In Fig. 3 it was observed that incrementing the order of the natural splines leads to an improvement in the performance of EMD. However, this is not a general conclusion as can be seen in Fig. 8 and particularly in the first and the second error bars where the example signal of Fig. 5 has been adopted and the 3rd and the 9th order splines have been used respectively. Observe that the higher order natural splines lead to an improved performance only when the frequency of the desired signal is at least twice the rest. In the next subsection, a GA-based optimization of the piecewise polynomials which form the upper and the lower envelopes will be realized while the interpolation points will stay fixed to the desired ones.

A. EMD optimization: Investigation on improved interpolation schemes

For the construction of the envelopes, e.g. the upper one, it is assumed that the corresponding interpolation points $x(\tau_{u,i})$, $1 \leq i \leq M$ are linked with $M-1$ 4th order polynomial curves[3] $P_i(t) = a_{u,i}t^4 + b_{u,i}t^3 + c_{u,i}t^2 + d_{u,i}t + e_{u,i}$, $\tau_{u,i} \leq t \leq \tau_{u,i+1}$. Moreover, the polynomials share the following properties

$$P_i(\tau_{u,i}) = x(\tau_{u,i}) \tag{13}$$

$$P_i(\tau_{u,i+1}) = x(\tau_{u,i+1}) \tag{14}$$

$$\frac{dP_i(t)}{dt}\Big|_{t=\tau_{u,i}} = \frac{dP_{i-1}(t)}{dt}\Big|_{t=\tau_{u,i}} \tag{15}$$

The continuity in the first derivative guarantees at least the minimum smoothness at the transitions between the polynomials at the interpolation points.

Each chromosome in the GA has $2 \times (L+M)$ genes $\chi = [D_{u,1}^{(1)}, \ldots, D_{u,L}^{(1)}, D_{u,1}^{(2)}, \ldots, D_{u,L}^{(2)}, D_{l,1}^{(1)}, \ldots, D_{l,M}^{(1)}, D_{l,1}^{(2)}, \ldots, D_{l,M}^{(2)}]$ which represent the values of the first and the second derivatives of the polynomials at the interpolation points, i.e.:

$$\frac{dP_i(t)}{dt}\Big|_{t=\tau_{u,i+1}} = D_{u,i+1}^{(1)} \tag{16}$$

$$\frac{d^2P_i(t)}{dt^2}\Big|_{t=\tau_{u,i+1}} = D_{u,i+1}^{(2)} \tag{17}$$

Equations (19)-(17) form $M-1$ linear systems of equations from which the unknown parameters $\{a_{u,i}, b_{u,i}, c_{u,i}, d_{u,i}, e_{u,i}\}$ and hence, the upper envelope can be easily computed. Using the last $2 \times M$

---

[3]The fourth order that is adopted here is not restrictive, and the same procedure could be realized with polynomials of higher or lower order.

genes of the chromosomes, the lower envelope can be computed in a similar way. The mean envelope is computed for all the chromosomes and their fitness is given by:

$$F = \int |M_{opt}^{(1)}(t) - m_1^{(1)}(t)| dt \tag{18}$$

Note that, in contrast to (10) a simpler fitness function is used here. In the case of the interpolation points optimization, the extra terms guaranteed that the interpolants would have an "envelope like" behaviour. Now that the subject of optimization is the envelopes themselves it is sensible to minimize the extraction error unaltered. The task of the GA is to search for the optimum derivatives that the piecewise polynomial should have at the interpolation points. Presumably, the derivative values determines the shape of the envelopes.

B. Novel interpolation methods

The above GA-based optimization procedure was applied on a portion, namely from 3000 to 4500 sec. of the multicomponent signal depicted in Fig. 5a which can be seen in Fig. 7 represented by the thick line. In the same figure, the thin line and the dashed line correspond to the upper envelope when it is constructed using natural cubic splines or the polynomials optimized by the GA respectively. It can
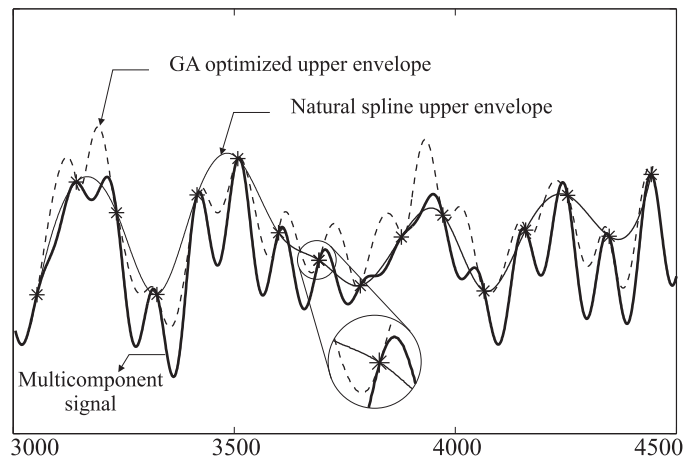

Fig. 7.   Upper envelope constructed either by natural cubic spline interpolation (thin curve) or by GA-optimized piecewise polynomial interpolation (dashed curve). The stars denotes the optimum interpolation points which have been adopted for the optimization procedure.

be observed that the difference in the behavior of the two envelopes. The spline envelope often crosses the signal, whereas the GA optimized envelope usually stays above it, and more importantly *it tends to be tangential to the signal at the interpolation points*, (which is indicated by the stars). In other words,

the first derivative of the envelope at the interpolation points coincide with that of the multicomponent signal.

The above observation brings directly to mind Hermite piecewise polynomial interpolation [21] which allows the determination of the value of derivatives at selected points. More specifically, in our case and kth order interpolation the following conditions are fulfilled in each knock $\tau_{.,i}$:

$$P_i(\tau_{.,i}) = P_{i+1}(\tau_{.,i}) = x(\tau_{.,i}) \tag{19}$$

$$\frac{dP_i(t)}{dt}\Big|_{t=\tau_{.,i}} = \frac{dP_{i+1}(t)}{dt}\Big|_{t=\tau_{.,i}} = \frac{dx(t)}{dt}\Big|_{t=\tau_{.,i}} \tag{20}$$

$$\frac{d^j P_i(t)}{dt^j}\Big|_{t=\tau_{.,i}} = \frac{d^j P_{i+1}(t)}{dt^j}\Big|_{t=\tau_{.,i}}, 2 \leq j \leq k \tag{21}$$
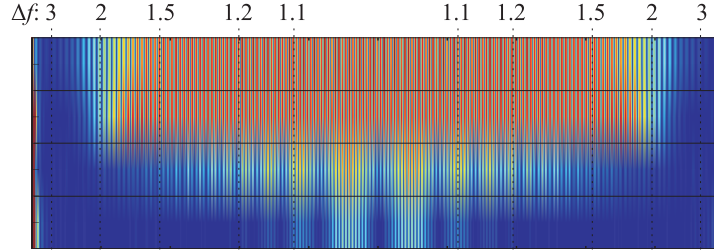

Fig. 8. Relative error corresponding to the first IMF extraction from signal of Fig. 5a when the desired interpolation points have been used. The first two error bars correspond to cubic and 9th order natural splines and the last two correspond to cubic and 5th order Hermite polynomial interpolation with estimated first derivatives.

The performance improvement that is achieved can be observed in Fig. 8. The first two error bars show the relative error when 3rd order and 9th order spline interpolation was used on the total length of signal shown in Fig.5a. The third error bar corresponds to the cubic Hermite interpolation with the first derivatives of the interpolation polynomials at the interpolation points set equal to the estimated first derivatives of the multicomponent signal. The fourth error bar corresponds to the 5th order Hermite interpolation where the derivatives higher than the first order are equal between the polynomial pieces in a similar manner to natural splines. In fact, the improvement is even better as the order of interpolation increases.

V. EVALUATION OF THE NEW TECHNIQUES

The findings of this paper are evaluated through studying four simulation examples. In all the cases, the extraction of the highest frequency signal is considered since the procedure is simply repeated after the extraction of each signal. As performance measure, the mean square error (MSE) between the extracted

IMF and the higher frequency signal, i.e., $MSE = \dfrac{1}{N_s} \sum\limits_{n=1}^{N_s} (h^{(1)}(n) - s(n))^2$ is adopted where N_s is the total number of samples and in general $s(n) = s_i(n)$, where i corresponds to the signal that has the higher frequency in the specific n. For simplicity here, the $s_1(t)$ has been always allowed to have the higher frequency along the time axis. Sampling frequency issues are not taken into account here [5], [22] and the multicomponent signal has been sampled at least 50 times faster than the Nyquist frequency. Moreover, when derivatives are needed, either for the extrema estimation or for the Hermite interpolation, they are estimated using (12).

A. Simulation Example I

(a) Original high frequency signal $s_1(t)$

(b) 3rd order Spline, (local extrema) - MSE=0.25

(c) 3rd order Hermite, (local extrema) - MSE=0.073

(d) 7th order Hermite, (local extrema) - MSE=0.020

(e) 13th order Hermite, (optimum extrema) - MSE=0.008

(f) 23th order Hermite, (optimum extrema) - MSE=0.001

(g) 13th order Hermite, (2nd derivative extrema) - MSE=0.009
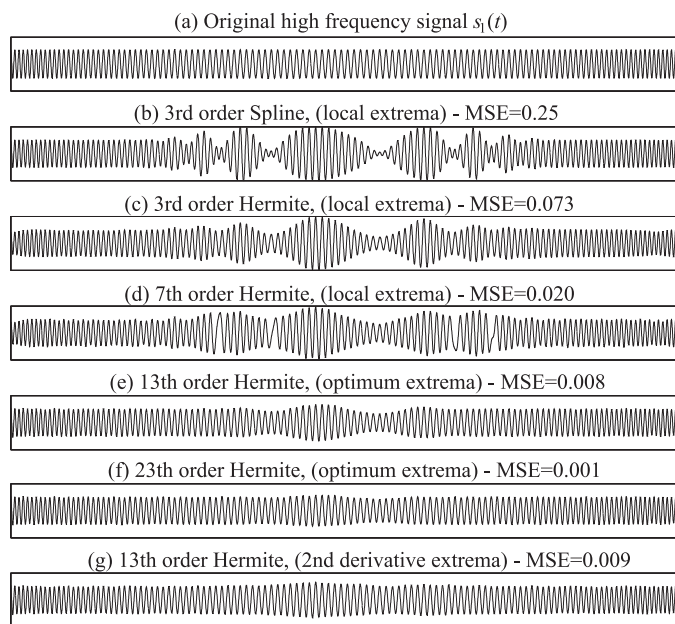
Fig. 9. The high frequency signal of the signal shown in Fig. 6a and its estimates provided by several configurations of EMD.

In this example, the multicomponent signal of Fig. 5a is used and concerns the extraction of signal $s_1(t)$, which is shown in Fig. 9a. In all the cases 500 sifting iterations have been applied. In Fig. 9b the results of the natural cubic splines and local extrema configuration of EMD which is the standard one used in the literature are shown. Fig. 9(c) corresponds to the scenario where Hermite interpolation was used instead of natural splines. The adoption of higher order Hermite interpolation (see Fig. 9d), and local extrema does not lead to better performance. However, when the desired interpolation points are used (Fig. 9(e)-(f)) each increment of the interpolation order leads to better decomposition performance. Remarkably, EMD with 23rd order Hermite interpolation and desired interpolation points succeeds in

separating signals that approach the other in frequency as close as $f_1 = 1.05 f_2$. Note that the separation which is achieved with natural splines and desired interpolation points regardless the interpolation order is accurate only for the frequency relation $f_1 < 2f_2$. Finally, for Fig. 9(g) EMD has not been provided with the optimum interpolation points but the second derivative of the multicomponent signal is used in each sifting iteration for their estimation. Observe that the performance of this setting approaches that with the desired interpolation points.

B. Simulation Example II

The high frequency resolution that the Hermite interpolation exhibits comes with a potential disadvantage in the cases of signals with relatively fast amplitude modulation. Lets take an example of a signal with sinusoidal AM, $x(t) = \cos(a(t)) \cos(\phi(t))$. Using product-to-sum trigonometric identities such a signal can also be equivalently written as $x(t) = \frac{1}{2} \cos(a(t) - \phi(t)) + \frac{1}{2} \cos(a(t) + \phi(t))$. As a result, it is a question of whether EMD is going to interpret a particular $x(t)$ as a single AM/FM signal or as two FM signals [9],[23]. Naturally, EMD supported by the high resolution provided from the Hermitian interpolation will tend to extract the two sinusoids separately, i.e. as different IMFs, particularly in the cases where the AM frequency is large enough in order to separate the two FM signal components significantly. The example of Fig. 10 explores such a scenario where the high frequency component along the time axis is formed by a constant FM signal amplitude modulated by a linear chirp 10(b). This signal is well separated in frequency with two other constant frequency signals together with which it forms the signal shown in Fig. 10(a). The error-bar (c1) correspond to the error between the signal in Fig. 10(b) and the first IMF, $h_1(t)$ extracted after 500 sifting iterations with 9th order Hermitian interpolants. Clearly, EMD succeeds in interpreting correctly only a small portion of the signal on the left of the time axis. However, after the extraction of the second IMF, $h_2(t)$, the initial AM/FM signal can be reconstructed as is shown in the error-bar (c2) where $h_1(t) + h_2(t)$ is compared with the signal in Fig. 10(a). If 150 sifting iterations are used instead, the behaviour of EMD remains the same. The EMD with natural cubic splines exhibits the same phenomenon but for much higher AM frequencies as can be seen in error-bars (d). In fact, the two corresponding FM signals are gradually separated in slower AM oscillations as the number of time siftings increases.

C. Simulation Example III

The signal adopted here is a *harsher* version of the multicomponent signal previously used in section III-C and is depicted in Fig. 11. The MSE on logarithmic scale with respect to sifting iterations is shown
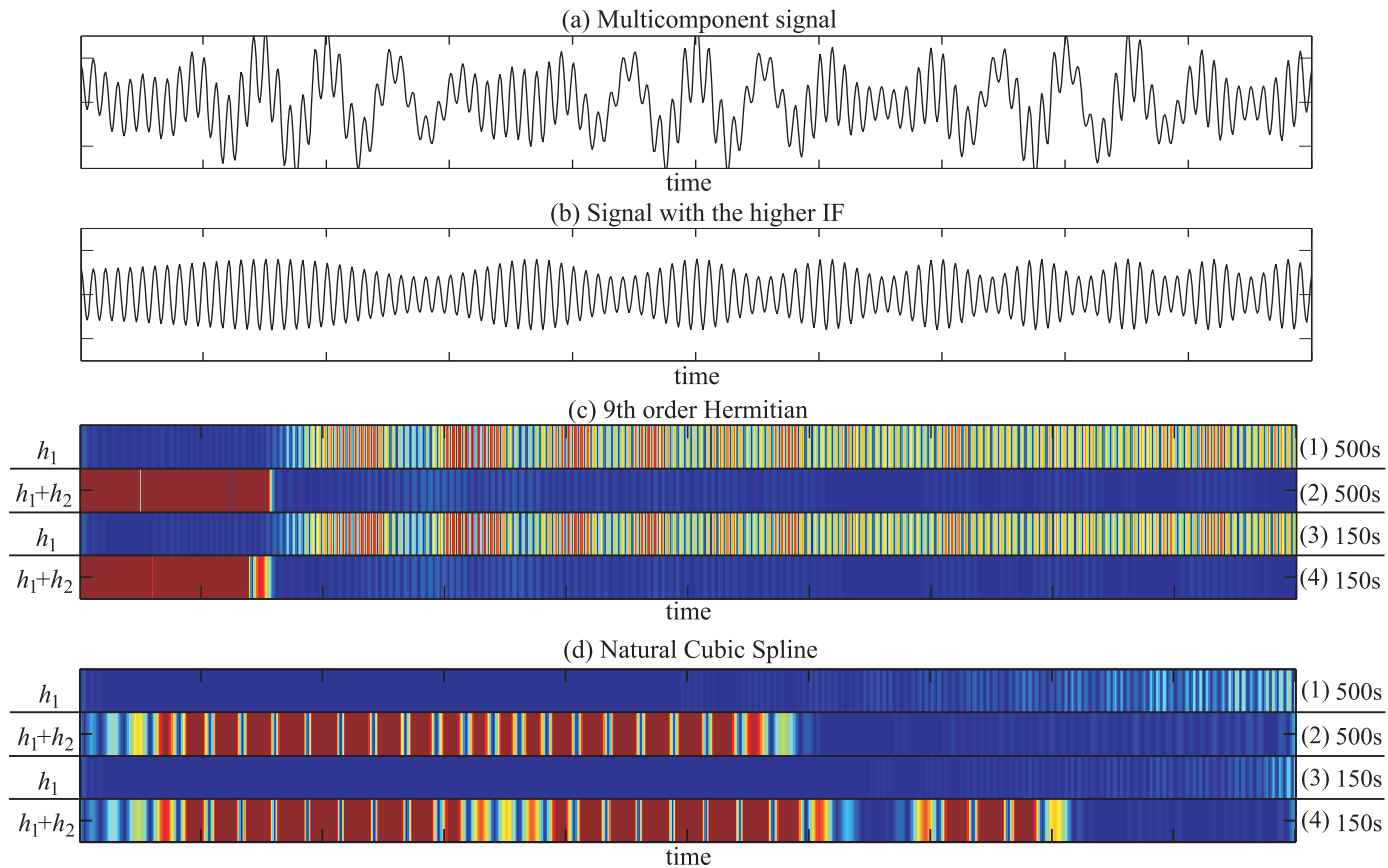
Fig. 10. The error-bars corresponding to the error between the high instantaneous frequency signal (b) and the first IMF or the sum of the two first IMFs produced after 150 or 500 siftings and interpolation methods 9th order Hermite (c) and natural cubic splines (d). The total multicomponent signal is shown in (a).

in Fig. 12 for a number of different configurations of the EMD method. In this figure, curves (1) to (5) correspond to desired interpolation points and the rest to the cases where the interpolation points were estimated from the local extrema of the multicomponent signal. In the cases of natural splines of order 3 and 7 (curves (1) and (2) respectively), the performance deteriorates with increasing order of the splines. In contrast, when Hermitian interpolation is used instead, the performance achieved is orders of magnitude better than with splines and it is enhanced with an increase in the interpolation order (curves (3) and (4)). Also observe, that the use of high order Hermite interpolation for a relatively short number of sifting iterations and then swapping to cubic Hermite interpolation leads to even better performance as shown in curve (5).

When the interpolation points are estimated from the local extrema, the spline method fails to decompose the signal and the cubic Hermite interpolation (curves (8) and (6) respectively) behave in a similar
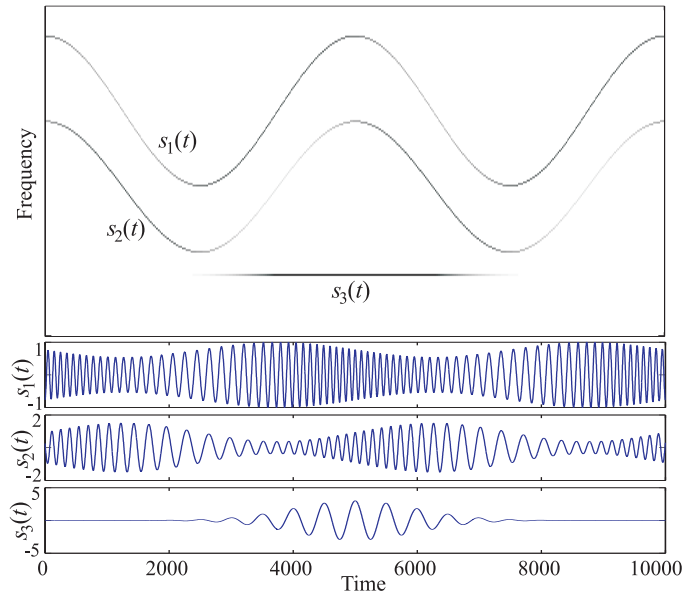
Fig. 11. Multicomponent signal used in simulation example III.

manner. However, for high order Hermite interpolation (polynomials of order 13) it performs very well and even outperforms the spline method with desired interpolation points as curve (7) shows. Unfortunately, in this simulation scenario better performance with the use of differentiation or FIR filtering was not achieved.

D. Simulation Example IV

In the last simulation example, two out of five signals that comprise the complex signal, are characterized by intrawave frequency modulation [1] given by

$$s(t) = \cos(2\pi f t + \epsilon \sin(2\pi f t)). \tag{22}$$

These signals are $s_1(t)$ and $s_4(t)$ as they are shown in Fig. 13 having $f = 1/150$, $\epsilon = 0.5$ and $f = 1/500$, $\epsilon = 0.7$ respectively. These kind of waves exhibit harmonic distortion similar to a Stokes wave producing a sharp crest and a rounded-off trough.

The MSE results with respect to sifting iterations are shown in Fig. 14. As far as the estimated extrema case is concerned, the estimates of the local extrema outperform the estimates from the derivative or the filtering methods. This happens not as a result of inaccurate estimates, but due to the fact that the intrawave frequency modulated signal of the high frequency signal was *translated* as a series expansion of different sinusoids. It is a phenomenon similar to that observed in the case of fast amplitude modulated signals.
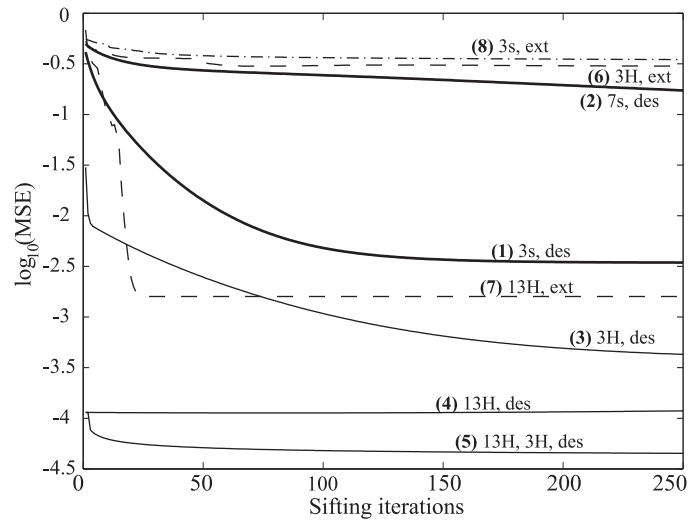
Fig. 12. MSE between the actual and the estimated highest frequency signal w.r. to the number of sifting iterations.
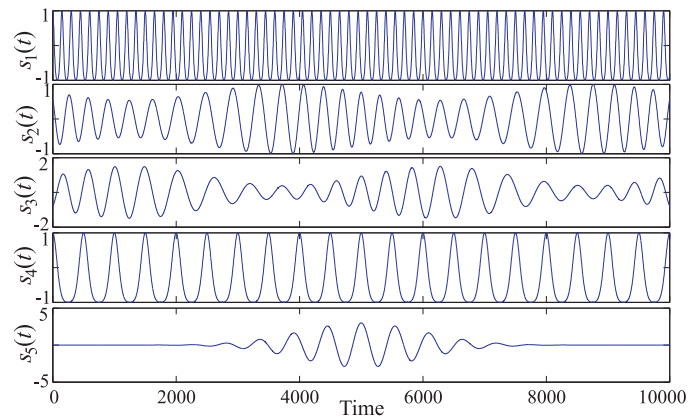

Fig. 13. Multicomponent signal containing intrawave frequency modulated signals.

With respect to interpolation points estimates via the multicomponent signal local extrema, as can be seen in curves (8)-(10) the cubic spline (curve (10)) method almost achieves the optimized case (curves (1) and (2)) and slightly outperforms the Hermite interpolation corresponding to curves (8) and (9). It seems that in this case, the Hermite interpolation method is more sensitive to the accuracy of the estimated extrema which force the EMD to decompose the intrawave frequency modulated signal into two parts.

It is very important to note that although the high frequency signal which is about to be extracted is nonlinear of the form described in equation 22, the behavior of the Hermite interpolation with the desired interpolation points (see curves (3)-(6)) remains the same as has been seen throughout the paper,
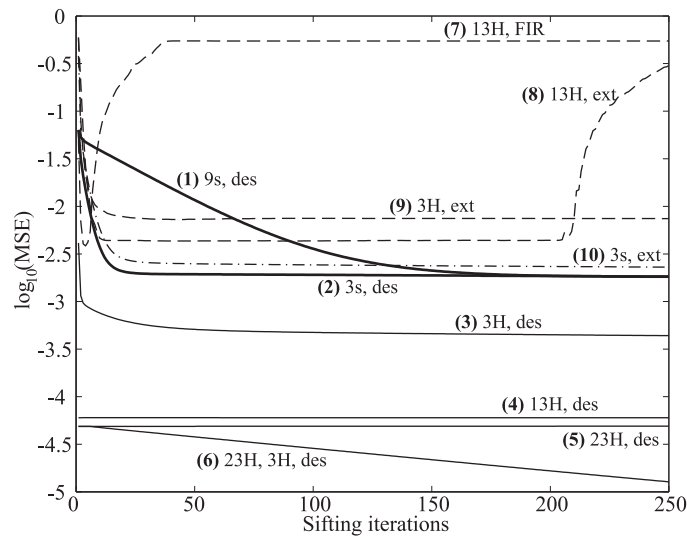
Fig. 14. MSE between the actual and the estimated by EMD first signal component w.r. to the number of sifting iterations.

i.e. exhibiting the best performance which is improved with an increase in the interpolation order. It is the view of the authors that further analytic investigation in this direction will add significantly towards a theoretical basis [10] for this promising decomposition technique.

E. Summarizing our understanding of EMD - Remarks on future research

There are some final clues to the actual function of EMD that can be now drawn based on both the GA-optimization and the simulation examples. As we saw, EMD attempts to iteratively approach a set of extrema which characterize the signal with the higher IF and EMD performance would appear to be maximized when the algorithm is supplied in each sifting iteration with the same desired extrema. Moreover, we have shown that the desired extrema can be approached by appropriate high-pass filtering operations. Our notion is that in each sifting iteration EMD performs a high-pass filtering operation on the signal under consideration reducing the energy of the signal components having lower frequencies. This in turn results in improved extrema estimates, i.e. local extrema closer to the desired ones. The next sifting iteration results in further filtered low frequency components and more accurate extrema estimates. An the same time, the high-pass filtering characteristics are such in order to prevent the fast oscillating signal from being filtered out. This is possible since the local extrema, on which the sifting iteration is based, mainly carries information about the fast oscillating signal. Very recent advances in the theoretical exploration of EMD [23] support analytically such a notion, namely a signal dependent high pass filtering process, for the sifting. Moreover, the EMD behaviour shown in Fig.10d supports the

findings reported in [23].

The interpolation method clearly plays an important role in the sifting process determining the frequency resolution that can be achieved. This is the difference between Hermitian interpolation and cubic splines interpolation. In terms of an equivalent iterative high-pass filtering process, the Hermitian interpolation might be translated to both higher cutoff frequencies and "steeper", i.e. closer to the optimum, filter shapes. From our point of view, the goal would be the development of interpolation methods which would have controlled and/or data-dependent resolution capabilities. The work in [24] is likely to provide directions for such a development.

Finally, the incorporation of the desired interpolation points as fixed will facilitate the analytical exploration of the method providing at the same time upper performance bounds. Furthermore, the cubic Hermitian interpolation is a local interpolation method in the sense that the corresponding piecewise polynomials depend only on the two nearest nodes. This renders the later interpolation method easier to handle mathematically than natural cubic splines.

VI. CONCLUSION

In this paper, the empirical mode decomposition algorithm was investigated from a novel perspective, that of a genetic algorithm based optimization. The approach facilitated a better understanding of the method and offered significant information about the interpolation points, the envelopes and their improved settings in several simulation examples. In this manner, a significant performance enhancement of EMD has been achieved. Moreover, the findings regarding the optimized interpolation points and envelopes will be useful in assisting the development of a more thorough mathematic analysis of EMD.

VII. ACKNOWLDEGMENTS

APPENDIX I

Consider a multicomponent signal comprising N constant amplitude and frequency sinusoids:

$$x(t) = \sum_{i=1}^{N} s_i(t) = \sum_{i=1}^{N} a_i \cos(2\pi f_i t), \tag{23}$$

where $f_1 > f_i$, $i = 2 \ldots N$ and its second derivative

$$x^{(2)}(t) = \frac{d^2 x(t)}{dt^2} = -4\pi^2 \sum_{i=1}^{N} a_i f_i^2 \cos(2\pi f_i t) \tag{24}$$

The time instances where the extrema of the high frequency signal $s_1(t)$ reside are given by $t_{s_1,k} = \frac{k}{2f_1}$, $k \geq 0$, i.e., the time instances where the first derivative of the signal becomes zero. Without loss of generality we are going to deal with the first extremum of the signal $t_{s_1,1} = 0$. For ease of notation purposes the value k will be omitted, i.e. $t_{s_1,0} \equiv t_{s_1}$. In other words, our analysis is restricted to the time interval $T = [-\frac{1}{4f_1}, \frac{1}{4f_1}]$. In the presence of the $N-1$ lower frequency signals $\sum_{i=2}^{N} s_i(t)$, the position of the extremum will shift from t_{s_1} with a deviation which depends on the first derivative of the latter sum. More specifically, the time instance t_x where the corresponding extremum may occur is given by

$$\frac{dx(t)}{dt}\Big|_{t=t_x} = 0 \Rightarrow$$

$$2\pi f_1 a_1 \sin(2\pi f_1 t_x) + 2\pi \sum_{i=2}^{N} f_i a_i \sin(2\pi f_i t_x) = 0 \Rightarrow$$

$$t_x = \frac{\arcsin\left(-\dfrac{\sum_{i=2}^{N} f_i a_i \sin(2\pi f_i t_x)}{a_1 f_1}\right)}{2\pi f_1} \tag{25}$$

In a similar way, the time instance $t_{x^{(2)}}$ that corresponds to the extremum of $x^{(2)}$ is given by

$$t_{x^{(2)}} = \frac{\arcsin\left(-\dfrac{\sum_{i=2}^{N} f_i^3 a_i \sin(2\pi f_i t_{x^{(2)}})}{a_1 f_1^3}\right)}{2\pi f_1} \tag{26}$$

It is easy to realise that each of the time instances in the interval T corresponds to a value between $[-1, 1]$ of the argument of the arcsin. Moreover, the time instances t_x and $t_{x^{(2)}}$ coincide with $t_{s_1} = 0$ when the argument of the arcsin is equal to zero and achieve their highest deviation from t_{s_1} for the values 1 or -1. In the cases where the absolute value of the argument of the arcsin is greater one, i.e. the arcsin is not defined, the corresponding extremum will be lost. In order to prove that the extrema of the second derivative of the signal are closer to the extrema of the high frequency signal than the ones of the signal itself it would be sufficient to show that

$$\left| \frac{\sum_{i=2}^{N} f_i a_i \sin(2\pi f_i t_x)}{a_1 f_1} \right| > \left| \frac{\sum_{i=2}^{N} f_i^3 a_i \sin(2\pi f_i t_{x^{(2)}})}{a_1 f_1^3} \right|. \tag{27}$$

Although (27) can not be guaranteed to be true, it can be proven that the maximum possible deviation between the optimized extrema and the extrema of the signal itself is always larger than the maximum possible deviation of the optimized extrema and the extrema of the second derivative of the signal. Taking into account that both f_i and a_i are positive, we can observe that $\dfrac{\sum_{i=2}^{N} f_i a_i \sin(2\pi f_i t_x)}{a_1 f_1} \leq \dfrac{\sum_{i=2}^{N} f_i a_i}{a_1 f_1}$ and $\dfrac{\sum_{i=2}^{N} f_i^3 a_i \sin(2\pi f_i t_{x^{(2)}})}{a_1 f_1^3} \leq \dfrac{\sum_{i=2}^{N} f_i^3 a_i}{a_1 f_1^3}$. In fact, these are the quantities that correspond to the highest possible deviation that can occur with the two methods. It can be easily shown that

$$\frac{\sum_{i=2}^{N} f_i^3 a_i}{a_1 f_1^3} \leq \frac{\sum_{i=2}^{N} f_i a_i}{a_1 f_1}, \tag{28}$$

or

$$\sum_{i=2}^{N} f_i f_1^2 a_i > \sum_{i=2}^{N} f_i^3 a_i, \tag{29}$$

which is valid since $f_1 > f_i$ for all $i > 1$.

REFERENCES

[1] N. E. Huang et. al., "The empirical mode decomposition and the hilbert spectrum for nonlinear and non-stationary time series analysis," *Proc. R. Soc. Lond. A*, vol. 454, pp. 903–995, Mar. 1998.

[2] L. Cohen, *Time-Frequency Analysis*. Prentice Hall, 1995.

[3] N. E. Huang and Z. Wu, "An adaptive data analysis method for nonlinear and nonstationary time series: The empirical mode decomposition and hilbert spectral analysis," in *The 4th International Conference on Wavelet Analysis and Its Applications (WAA 2005)*, 2005.

[4] G. Rilling, P. Flandrin, and P. Gonçalvès, "On empirical mode decomposition and its algorithms," in *IEEE Workshop on Nonlinear Signal and Image Processing, NSIP 2003.*, 2003.

[5] G. Rilling and P. Flandrin, "On the influence of sampling on the empirical mode decomposition," in *IEEE International Conference on Acoustics, Speech and Signal Processing, ICASSP 2006*, vol. 3, 2006, pp. 444–447.

[6] H. Liang, Q.-H. Lin, and J. D. Z. Chen, "Application of the empirical mode decomposition to the analysis of esophageal manometric data in gastroesophageal reflux disease," *IEEE Trans. Biomed. Eng.*, vol. 10, pp. 1692– 1701, Oct. 2005.

[7] B. Liu, S. Riemenschneider, and Y. Xu, "Gearbox fault diagnosis using empirical mode decomposition and Hilbert spectrum," *Mechanical systems and signal processing (Elsevier)*, vol. 20, pp. 718–734, 2006.

[8] K. T. Coughlin and K. K. Tung, "11-Year solar cycle in the stratosphere extracted by the empirical mode decomposition method," *Adv. Space. Res.*, vol. 34, pp. 323–329, 2004.

[9] R. Deering and J. F. Kaiser, "The use of a masking signal to improve empirical mode decomposition," in *IEEE International Conference on Acoustics, Speech and Signal Processing, ICASSP 2005*, vol. 4, 2005, pp. 485–488.

[10] N. E. Huang and S. Shen, *Hilbert-Huang Transform and Its Applications*, 1st ed. World Scientific Publishing Company, 2005.

[11] E. Deléchelle, J. Lemoine, and O. Niang, "Empirical mode decomposition: An analytical approach for sifting process," *IEEE Signal Processing Lett.*, vol. 12, pp. 764– 767, Nov. 2005.

[12] Q. Chen, N. Huang, S. Riemenschneider, and Y. Xu, "A b-spline approach for empirical mode decompositions," *Advances in Computational Mathematics*, vol. 24, pp. 171–195, Nov. 2006.

[13] P. Flandrin, G. Rilling, and P. Goncalves, "Empirical mode decomposition as a filter bank," *IEEE Signal Processing Lett.*, vol. 11, pp. 112– 114, Feb. 2004.

[14] V. J. Rayward-Smith, I. H. Osman, C. R. Reeves, and G. D. Smith, *Modern Heuristic Search Methods*, 3rd ed.   John Wiley Sons, 1996.

[15] K. S. Tang, K. F. Man, S. Kwong, and Q. He, "Genetic algorithms and their applications," *IEEE Signal Processing Mag.*, pp. 22–37, Nov. 1996.

[16] N. E. Huang, Z. Shen, and S. R. Long, "A new view of nonlinear water waves: The hilbert spectrum," *Annu. Rev Fluid. Mech*, vol. 31, pp. 417–457, 1999.

[17] N. E. Huang et. al., "A confidence limit for the empirical mode decomposition and hilbert spectral analysis," *Proc. R. Soc. Lond. A*, vol. 459, pp. 2317–2345, 2003.

[18] W. H. Press, *Numerical Recipes in C : The Art of Scientific Computing*.   Cambridge University Press, 1992.

[19] M. Hasson, "Wavelet-based filters for accurate computation of derivatives," *Mathematics of Computation*, vol. 75, no. 253, pp. 259–280, 2005.

[20] J. Pittman, "Adaptive splines and genetic algorithms," *Journal of Computational and Graphical Statistics*, vol. 11, pp. 615–638, 2002.

[21] C. Pozrikidis, *Numerical Computation in Science and Engineering*, 1st ed.   Oxford University Press, 1998.

[22] N. Stevenson, M. Mesbah, and B. Boashash, "A sampling limit for the empirical mode decomposition," in *8th International Symposium on Signal Processing and Its Applications, ISSPA 2005*, vol. 2, 2005, pp. 647–650.

[23] G. Rilling and P. Flandrin, "One or two frequencies? the empirical mode decomposition answers," *submitted to IEEE trans. on Signal Proc.*, vol. web:http://prunel.ccsd.cnrs.fr/ensl-00113834.

[24] Y. Washizawa, T. Tanaka, D. P. Mandic, and A. Cichocki, "A flexible method for envelope estimation in empirical mode decomposition," in *Knowledge-Based Intelligent Information and Engineering Systems, 10th International Conference, KES 2006, Bournemouth, UK*, 2006.